

Mapping Subsurface Alteration Using Gravity and Magnetic Inversion Models

Williams, N. ^[1], Dipple, G. ^[1]

1. Mineral Deposit Research Unit, Department of Earth and Ocean Sciences, The University of British Columbia, Canada

ABSTRACT

Inversions of geophysical data are becoming routine components of mineral exploration programs and can provide acceptable subsurface physical property models that can be interpreted in terms of the geometry and relative sizes and intensities of physical property anomalies. The only available link to actual geological interpretation of such models is a large database of physical property measurements on the rocks within the inversion volume. A more robust method for interpreting physical properties is to estimate the abundance of expected minerals within the rocks based on the physical properties of the rocks, the physical properties of the minerals and an understanding of the ore deposit models appropriate for the rocks of interest. For most basement rocks the magnetic susceptibility and density of a sample are linearly related to the susceptibility and density of the constituent minerals. Measured or predicted susceptibilities and densities can therefore be used to identify and quantify the presence of minerals, especially sulphides, which have anomalous physical properties. With selection of appropriate minerals and their physical properties, and using linear programming techniques, we can extract estimates of mineral abundances from drill core property measurements or 3D inversion property models where the minerals of interest have significantly different physical properties from the host rocks. Property measurements from the Perseverance komatiite-hosted nickel-sulphide deposit in Western Australia are used to test the mineral estimates against independent assessments of the mineralisation in the samples. The results provide realistic estimates of the possible range of Ni-bearing pentlandite in each sample; > 80 % of samples with known anomalous sulphide content were identified from their physical properties alone. Application of this procedure, with a different set of end-members, to geologically-constrained gravity and magnetic inversion models from the Olympic Fe-oxide Cu-Au province in South Australia demonstrates how it can be used to map, in 3D, areas of potentially anomalous sulphide accumulation to aid exploration and target selection.

INTRODUCTION

Inversion of potential field data can readily provide models of the distribution of physical properties in the subsurface, but rigorous geological interpretation of those property models is challenging. For mineral exploration, qualitative interpretations may be based on associations expected for mineralisation or alteration, such as the existence of “coincident magnetic and density anomalies”. However, there is merit in assessing prospectivity more rigorously. Cross-plots of measured densities and susceptibilities can be used to help classify rock types and general alteration trends (Henkel, 1976; Puranen, 1989; Henkel, 1994), and can provide some rapid insights into the rock characteristics and allow some broad classifications. However they only provide a graphical rather than a quantitative approach. Cluster analysis techniques provide a more quantitative method for classifying rock types and alteration trends, but do not allow for any direct inclusion of information about geological processes and characteristics.

Quantitative methods for estimating mineralogy from remotely acquired reflectance spectra have been in use for

more than two decades (Smith et al., 1985). These spectral unmixing techniques assume that a pixel’s observed reflectance spectra are linearly related to the abundance of various end-member components within that pixel and use inversion to extract the component abundances from the observed band reflectances (Van der Meer and De Jong, 2000). Two of the most troublesome issues with spectral unmixing techniques are selecting the appropriate end-member components (Theseira et al., 2003) and correlation or similarity between end-member responses (Van der Meer and De Jong, 2000) and various strategies have been proposed to mitigate these problems.

The unmixing approach may be applied to other data types, such as the densities and magnetic susceptibilities that are among the most commonly used geophysical datasets in mineral exploration. When limited to only two data, density and susceptibility, instead of multiple spectral bands the number of end-member components that can be uniquely resolved becomes severely limited. One mitigation strategy, known as partial unmixing, is to only extract the abundances of those end-member components that are most relevant for the questions being addressed (Boardman et al., 1995). All other components are lumped together as a single component containing everything else (Boardman et al., 1995); in our implementation to follow this

component will be the “host rock”. This method is particularly appropriate for densities and susceptibilities as most common rock-forming minerals have very similar densities and susceptibilities. Extremely high densities and susceptibilities are generally due to the sulphides and oxides that are of direct importance to mineral exploration. This association also provides us a better understanding of which end-member components need to be included in the unmixing calculation, thus eliminating the need for complex component selection algorithms.

For Fe-oxide Cu-Au (IOCG) systems, Hanneson (2003) assumed that the physical properties of any rock were controlled by the abundance and physical properties of three end-member components: magnetite, combined hematite and sulphides, and the host rock (a fictitious pure end-member that contains no magnetite, hematite, or sulphides). He could then solve a simple system of three weakly non-linear equations for the abundance of each of the three end-members

$$\kappa_{mgt} f_{mgt}^{\phi} + \kappa_{hem} f_{hem} + \kappa_{host} f_{host} = \kappa_{sample} \quad (1)$$

$$\rho_{mgt} f_{mgt} + \rho_{hem} f_{hem} + \rho_{host} f_{host} = \rho_{sample} \quad (2)$$

$$f_{mgt} + f_{hem} + f_{host} = 1 \quad (3)$$

where κ is susceptibility, ρ is density, and f is the volume fraction of the component (from 0 to 1), κ_{sample} is the susceptibility of the sample, ρ_{sample} is the density of the sample, and ϕ is an empirical exponent that has been variously estimated at between 1.0 and 1.39 depending on the value of κ_{mgt} , the grain size of magnetite in the sample, and the method used for estimating f_{mgt} (see compilation by Schön, 2004).

Williams et al. (2004) showed that this method can be applied directly to the 3D density and susceptibility models derived from constrained gravity and magnetic inversions to map, in 3D, regions of anomalous hematite or sulphide accumulations which may be prospective for exploration. The physical properties included in a constraining reference model supplied to the gravity and magnetic inversions are used to derive the properties expected for barren host rock within each mappable rock unit. For each inversion cell, the density and susceptibility recovered by the inversions is used to estimate the abundance of each of the three end-member components by solving the system of three equations outlined above and in

Figure 1. The results can then be displayed as 3D maps of magnetite, hematite and sulphide, or barren host rock abundance.

This method may provide an acceptable first pass estimate of sulphide abundance for many sulphide-rich deposit styles, but there are several deficiencies with this approach. One is that many more minerals contribute to the physical properties of the rocks than the three end-member system allows. Sericite alteration is common in volcanic hosted massive sulphide (VHMS) and IOCG systems and the ultramafic host rocks in many nickel sulphide deposits are strongly serpentinised. These low density phases complicate the systematics of the three-end-member mineralogy estimate by introducing a component that may have a lower density than the allowed host rock density. Such rocks have no possible solution in the three-end-member system (grey triangle in

Figure 1). There may also be a range in the physical properties of each end-member mineral, or the properties of each mineral may be poorly known. The uncertainty associated with the physical properties recovered from inversions is also not taken into account.

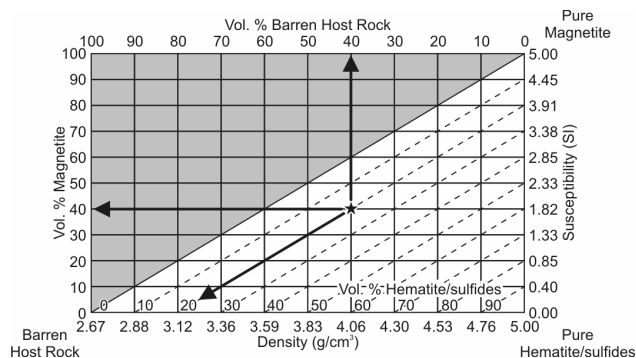


Figure 1: Graphical representation of the equations 1-3 depicting how the density and susceptibility of a sample may be used to estimate the volume proportions of each of three end-members. Valid solutions are only possible in the white triangle. Modified from Hanneson (2003).

To address these issues, a new method of estimating mineralogy from physical properties is developed here. The method follows the approach of Gordon and Dipple (1999) who applied linear programming techniques to estimate mineral abundances from whole rock chemistry compositions. Although not intended to replace direct observation, we first demonstrate the applicability of our mineralogy unmixing method to different deposit styles, and test its accuracy, by applying it to actual measured densities and susceptibilities for drill core samples from the Perseverance komatiite-hosted nickel sulphide deposit in Western Australia’s Archean Yilgarn Craton. We then apply the technique to the results of regional-scale geologically-constrained inversions (originally developed by Williams et al., 2004) around the Olympic Dam IOCG deposit in South Australia’s Proterozoic Gawler Craton to assess the method’s use in targeting and ranking prospective targets for exploration at depth and under cover.

METHOD

If the volume fraction of magnetite in a sample is less than about 0.1 (or 10 volume %), the empirical exponent ϕ in equation 1 contributes little and the system is approximately linear (Clark, 1997). Even for samples with > 0.1 volume fraction magnetite, a linear approximation only overestimates the abundance of magnetite slightly. For this reason, and the complexity and instability of nonlinear implementations (using quadratic programming methods), the linear approximation is deemed adequate. The general linear approximation of the system for n end-member components is

$$\sum_{i=1}^n \kappa_i f_i = \kappa_{sample} \quad (4)$$

$$\sum_{i=1}^n \rho_i f_i = \rho_{sample} \quad (5)$$

$$\sum_{i=1}^n \rho_i f_i = 1 \quad (6)$$

where κ_i and ρ_i are the susceptibility and density of mineral or component i , f_i is the volume fraction of mineral or component i , and κ_{sample} and ρ_{sample} are the sample susceptibility and density. Thus when $n > 3$ the system is underdetermined and an exact solution for f cannot be obtained. In such underdetermined problems optimisation techniques can be applied to seek preferred solutions. Our use of linear programming is based on that presented by Gordon and Dipple (1999).

LINEAR PROGRAMMING

Linear programming is an optimisation method that seeks a solution that minimises some linear objective function subject to a finite number of linear inequality constraint equations. The inequality equations define an n -dimensional convex feasible region, or polytope, the vertices of which provide the set of possible solutions for the optimisation problem. The vertex that minimises the objective function is the optimal solution. For linear programming the standard form of equations is

$$\min_{\mathbf{x}} F(\mathbf{x}) \text{ such that } \begin{cases} \mathbf{Ax} \leq \mathbf{b} \\ \mathbf{lb} \leq \mathbf{x} \leq \mathbf{ub} \end{cases} \quad (7)$$

where $F(\mathbf{x})$ is an objective function of the unknowns, \mathbf{x} , of the form:

$$F(\mathbf{x}) = \mathbf{c}^T \mathbf{x} = c_1 x_1 + c_2 x_2 + \dots + c_n x_n \quad (8)$$

A is a matrix of coefficients to a set of inequality equations, \mathbf{b} represents limiting values, \mathbf{lb} and \mathbf{ub} are vectors of the lower and upper bounds on possible values of \mathbf{x} , and \mathbf{c} is a vector of coefficients defining the objective function.

Many linear programming algorithms are freely or commercially available. Throughout this work we use the CDD linear programming algorithm developed by Fukuda and Prodon (1996) after Motzkin et al. (1953) and interfaced to the Matlab software package (Mathworks Inc., Natick, Massachusetts) as CDDMEX by Torrisi and Baotic (2005).

Inequality constraint equations

To be included in the linear programming routine, the equality equations 4-6 must be transformed into the form $\mathbf{Ax} \leq \mathbf{b}$ used in the linear programming equation 7. From equations 4-6 and using the procedure of Gordon and Dipple (1999), we derive the six inequality equations

$$-\sum_{i=1}^n \kappa_i^{\max} \cdot f_i \leq -\kappa_{sample}^{\min} \quad \text{and} \quad \sum_{i=1}^n \kappa_i^{\max} \cdot f_i \leq \kappa_{sample}^{\max} \quad (9)$$

$$-\sum_{i=1}^n \rho_i^{\max} \cdot f_i \leq -\rho_{sample}^{\min} \quad \text{and} \quad \sum_{i=1}^n \rho_i^{\min} \cdot f_i \leq \rho_{sample}^{\max} \quad (10)$$

$$-\sum_{i=1}^n f_i \leq -(1 - \Delta v) \quad \text{and} \quad \sum_{i=1}^n f_i \leq (1 + \Delta v) \quad (11)$$

These are the fundamental equations used to calculate the mineral abundances and can readily be written in the $\mathbf{Ax} \leq \mathbf{b}$ form required for linear programming algorithms, with \mathbf{x} being a vector of the unknown component abundances f_i . The minimum and maximum susceptibility for each mineral or component are κ_i^{\min} and κ_i^{\max} , and the minimum and maximum densities are ρ_i^{\min} and ρ_i^{\max} . The minimum and maximum sample densities and susceptibilities of the form ρ_{sample}^{\min} and ρ_{sample}^{\max} reflect the range of observed values for a sample; typically these may be defined in terms of ± 2 standard deviations of measurements. The uncertainty defined by Δv allows the volume sum to vary within an appropriate number of significant figures; we set it to 0.001 or 0.1 vol. %.

Since the problem is underdetermined, the solution space may be infinitely large, and extra constraints may help refine the solution. The types of constraints available will vary depending on the deposit style and end-member components used, but will typically be based on limitations imposed by an understanding of the petrography and expected relationships between the minerals that might arise given a particular alteration or mineralisation style; this can come directly from ore deposit models. To be included in the calculation the constraints must be of the form $\mathbf{Ax} \leq \mathbf{b}$ and will generally be based on observations of the form: "alteration minerals are more abundant than ore minerals," or "mineral A is always more common than mineral B," or "the abundance of mineral A is proportional to the abundance of mineral B." Specific examples will be given with the examples below.

In most linear programming implementations the lower and upper bounds on \mathbf{x} are supplied to the linear programming algorithm as two vectors. The algorithms then transform the bounds vectors into addition inequality constraints of the form

$$-x_i \leq -lb_i \quad \text{and} \quad x_i \leq ub_i \quad (12)$$

Model objective function

Every vertex of the polytope defined by the inequality constraint equations outlined above is a valid solution to the optimisation problem. The optimal solution returned by the linear programming algorithm is defined by the vertex that minimises the supplied objective function $F(\mathbf{x})$, so selection of an appropriate objective function is critical in recovering useful mineral estimates.

Due to the underdetermined nature of the mineral estimation problem for more than 3 components, an exact solution cannot be

obtained. It is therefore unreasonable to expect the linear programming routine to provide a single ideal solution. Instead it is useful to define two objective functions that define the likely range of possibilities for a particular problem. For mineral exploration, an appropriate pair of objective functions would seek to minimise and maximise the abundance of ore sulphides thus providing an estimate of the range of ore sulphide abundances. Another pair of objective functions might seek to minimise and maximise the abundance of a particular alteration phase.

By only seeking the possible range of mineral abundances, rather than an exact solution, many more end-member components can be included in the unmixing calculation than the three equations allow; however, as the number of components increases and the problem becomes more underdetermined, the extracted range of mineral abundances will widen, possibly reducing the effectiveness of the estimate. Therefore it remains important to select only those end-member components that are most likely to control the physical properties of the rocks; this decision is best based on a geological understanding of the rocks. The abundance of minor phases not included in the calculation will add some small error to the calculated ranges of mineral abundances.

Standard linear programming algorithms minimise an objective function of the form shown in equation 8. Maximising the value of an unknown component abundance, x_i , is equivalent to minimising the value of $-x_i$. The coefficients, c_i , in the objective function equation 8 are therefore +1 or -1 depending on whether that component should be minimised or maximised respectively.

APPLICATION TO DRILL CORE SAMPLES

To demonstrate how the mineral estimates are obtained, and their accuracy, we first apply the method to a set of 144 drill core and surface samples from the Leinster komatiite-hosted nickel sulphide deposits. The Leinster group includes the Perseverance, Rocky's Reward, and Harmony deposits which contain massive nickel sulphide basal horizons, disseminated intercumulus nickel sulphides, and tectonically remobilised sulphides, with a total underground resource of 33 Mt at 2.3 wt. % Ni and an open pit resource of 155 Mt at 0.6 % Ni (BHP Billiton Ltd., 2006). The sulphides are generally hosted within variously serpentinised Archean ultramafic cumulate and flow rocks within a regionally extensive greenstone belt that also includes basaltic and gabbroic rocks, felsic porphyry, volcanic and volcanoclastic rocks, and sedimentary rocks that have all been metamorphosed up to amphibolite grade (Gole et al., 1989; Libby et al., 1998). The greenstone belt is bounded by regional-scale fault systems which juxtapose the greenstones against several suites of voluminous granitoid rocks. The samples represent all major rock types in the area and all styles of nickel sulphide mineralisation, from weakly disseminated sulphides and sulphide stringers in ultramafic rocks to massive sulphides. Although detailed petrographic analysis of all the samples has not yet been completed, each sample has been visually classified in terms of its host rock, alteration styles, and sulphide abundance and style.

To measure densities, the samples were dried for two days at 110 °C, weighed, soaked in water for two days, weighed, and then weighed suspended in water. The susceptibility of each sample is the geometric mean of the susceptibilities of three 22 mm × 22 mm × 22 mm cubes that were analyzed on either a Digico susceptibility bridge (for lower susceptibilities) or an AGICO KLY-3 kappabridge (for higher susceptibilities). Measured densities and susceptibilities for each sample were compared to the observed sample mineralogy to ensure that the measurements showed appropriate magnitudes.

Components, their properties and bounds

The densities and susceptibilities are plotted in Figure 2 with the seven components that are most likely to control the physical properties in such rocks: magnetite, serpentine, monoclinic pyrrhotite, pyrite, the nickel ore pentlandite, and barren host rock. It is noted that many other minerals with extreme physical properties may be present in small amounts, including chalcopyrite, ilmenite, chromite, and millerite, but their total abundance is generally < 2 vol. % and their exclusion will only add an equivalently small error to the result. In fact, many of these components will effectively be included in the estimates of other mineral components with similar properties: ilmenite and chromite will likely be included in the pyrite estimate; chalcopyrite will be partially included in the pentlandite estimate.

The extents of the boxes in Figure 2 indicate the range of expected properties for each component. The minerals' properties are based on published literature values (

Table 1). The density range allowed for the barren host rock component spans the range of densities observed for least-altered lithologies in the area regardless of rock type; the susceptibility range for the barren host rock component extends to 7×10^{-3} SI, the typical upper limit of rocks lacking ferrimagnetic minerals (Clark, 1997).

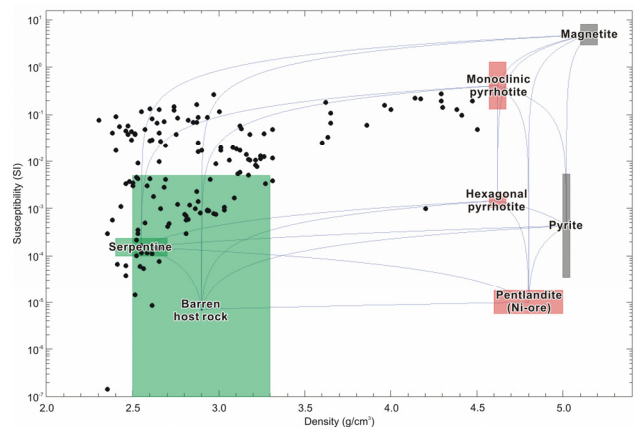


Figure 2: Densities and magnetic susceptibilities of the 144 drill core samples in this study (black circles), and seven controlling components. Blue lines represent linear mixing lines between the geometric mean properties of each of the components – they appear curved because of the logarithmic susceptibility scale.

Table 1: Summary of the physical properties of the components that will control the physical properties of rocks associated with komatiite-hosted nickel sulphide deposits. Where conflicting ranges are reported in the literature, a representative range is used.

Mineral	Minimum density (g/cm ³)	Maximum density (g/cm ³)	Minimum susceptibility (SI)	Maximum susceptibility (SI)	References
Barren host rock (allows for all likely host rock types)	2.5	3.3	1.00 × 10 ⁻⁸	7.00 × 10 ⁻³	Densities based on physical property measurements in this study; susceptibilities based on diamagnetic and paramagnetic minerals (Clark, 1997)
Serpentine	2.40	2.70	9.88 × 10 ⁻⁵	2.38 × 10 ⁻⁴	Chesterman and Lowe (1979), Bleil and Petersen (1982), Wohlenberg (1982)
Pyrite	5.00	5.04	3.50 × 10 ⁻⁵	5.27 × 10 ⁻⁴	Carmichael (1982), Hunt et al. (1995)
Pentlandite	4.60	5.00	5.62 × 10 ⁻⁶	1.78 × 10 ⁻⁵	Wohlenberg (1982), Emerson et al. (1999)
Hexagonal pyrrhotite (Fe ₉ S ₁₀)	4.57	4.67	1.05 × 10 ⁻³	2.01 × 10 ⁻³	Hunt et al. (1995), Emerson et al. (1999)
Monoclinic pyrrhotite (Fe ₇ S ₈)	4.57	4.67	0.13	1.30	Hunt et al. (1995), Clark (1997)
Magnetite	5.10	5.20	3	8	Telford et al. (1990), Clark (1997)
Term in equations 9 and 10	ρ_i^{\min}	ρ_i^{\max}	κ_i^{\min}	κ_i^{\max}	

Table 2: Expected minimum and maximum abundances of each mineral for rocks from the Leinster area.

Mineral	Abbreviation	Minimum abundance (vol. fraction)	Maximum abundance (vol. fraction)
Serpentine	serp	0.0	1.0
Pyrite	py	0.0	0.15
Pentlandite	pen	0.0	0.3
Hexagonal pyrrhotite	poH	0.0	1.0
Monoclinic pyrrhotite	poM	0.0	1.0
Magnetite	mgt	0.0	0.1

Our goal for these samples is to estimate the possible range of sulphide abundance in each sample and compare the estimates to visual estimates of sulphide abundance to assess the effectiveness of the mineral estimates at classifying sulphidic rocks as anomalous. Once the relevant components expected in the samples have been identified (above;

Table 1), the next step is to identify the expected minimum and maximum abundance of each in the dataset. In general these may be 0.0 and 1.0 respectively (0 to 100 vol. %), but in many situations more restrictive ranges may be expected as shown for Leinster in Table 2. These values reflect many of the more extreme rocks that might exist; most rocks are unlikely to contain 100 vol. % serpentine or hexagonal or monoclinic pyrrhotite, so these upper and lower bounds are relatively loose.

Objective functions

We then define the two objective functions that will be used to extract the range of feasible solutions. For nickel exploration we are most interested in the abundance of the nickel ore pentlandite, so we will select one objective function to extract the mineralogy containing the maximum possible abundance of pentlandite (all $c_i = +1$ are minimised, except $c_{pen} = -1$ is maximised)

$$F_1(\mathbf{x}) = \mathbf{c}^T \mathbf{x} = x_{mgt} - x_{pen} + x_{poH} + x_{poM} + x_{py} + x_{serp} + x_{host} \quad (13)$$

The second objective function will reproduce a barren host rock with as few sulphides as possible by maximising the volume fraction of barren host rock present in each sample

$$F_2(\mathbf{x}) = \mathbf{c}^T \mathbf{x} = x_{mgt} + x_{pen} + x_{poH} + x_{poM} + x_{py} + x_{serp} - x_{host} \quad (14)$$

Additional constraint equations

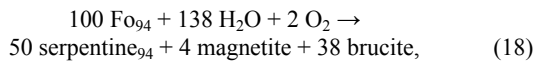
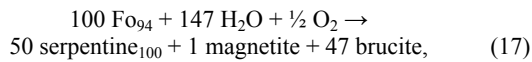
Several additional constraints are available that can be included in the formulation. For this example the information comes from knowledge of the typical sulphide mineral assemblage and the serpentinisation reaction observed in the ultramafic rocks. Previous workers have reported typical pyrrhotite to pentlandite ratios of 3:1 (Martin and Allchurch, 1975), 7.5:1 (Emerson et al., 1999) and 11.5:1 (Duuring et al., 2007) for the Leinster nickel deposits. To encapsulate this range of variability in reported ratios we define a range of pyrrhotite to pentlandite ratios from 1:1 to 15:1 with the following two constraint equations

$$x_{pen} \leq x_{poH} + x_{poM} \quad (15)$$

$$15x_{pen} \geq x_{poH} + x_{poM} \quad (16)$$

which can in turn be included with equations 9-11 as two extra rows in the linear programming equation 7.

Most of the rocks that host mineralisation are ultramafic rocks that have undergone varying degrees of serpentinisation whereby primary igneous olivine is replaced by serpentine and magnetite in the presence of fluids. Barnes et al. (1988) report that primary igneous olivine at Leinster has an average composition of $F_{0.94}$ (Mg-number = $100 \times \text{MgO}/[\text{MgO}+\text{FeO}] = 94$). Such Mg-rich olivine is likely to hydrate to Mg-rich serpentine plus minor magnetite. Without electron microprobe analyses of the serpentine at Leinster, two possible balanced serpentinisation reactions that provide a minimum and maximum amount of magnetite produced might be



where Fo_{94} represents the primary igneous olivine, serpentine_{100} and serpentine_{94} represent serpentine with Mg-numbers of 100 and 94 respectively. Brucite $[\text{Mg}(\text{OH})_2]$ is a common alteration by-product of serpentinisation but has a similar density to serpentine (Wohlenberg, 1982) so for the mineral estimation calculations it is treated as part of the serpentine component. For each of these two equations the molar ratio of [(serpentine + brucite) / magnetite] can be converted to a mass ratio and then a volume ratio of [(serpentine + brucite) / magnetite] to define an approximate range of such ratios that is possible. Assuming that the alteration system is closed (no net mass or elemental loss), and that the compositions specified in reactions 17 and 18 represent the full compositional range of the minerals, then this calculation provides a range of serpentine to magnetite volume ratios that can be expressed as

$$35x_{\text{mgt}} \leq x_{\text{serp}}, \quad (19)$$

$$150x_{\text{mgt}} \geq x_{\text{serp}}, \quad (20)$$

again, assuming that all brucite is included in the serpentine component. These two equations can also be added as additional rows with equations 9-11 in the linear programming equation 7.

In the mineral estimation calculation we provide no information regarding rock type or whether serpentinisation is present. Instead, by providing these constraints we are assuming that magnetite is only significant (>1 vol. %) in those samples where serpentinisation of ultramafic rocks has taken place. Where no serpentinisation has taken place but minor magnetite is present, such as in a granitic sample, this assumption fails and the calculation may give rise to an erroneous proportion of serpentine which, due to its low density, may allow an erroneous estimate of sulphide content resulting in a false positive anomaly. However, nearly all of the sulphides are hosted in serpentinised ultramafic rocks, and this constraint is critical in correctly identifying sulphides in these samples.

Results

The equations, objective functions, and the 144 rock samples' property measurements are supplied directly to the linear programming routine as matrices. The results are presented in Figure 3. Each vertical bar represents one of the 144 individual rock samples. The bars are coloured by their actual sulphide content, either barren, trace disseminated sulphides, moderate disseminated sulphides, heavy disseminated sulphides, and massive sulphides. The tops and bottoms of each bar represent the solutions extracted using each of the two objective functions. The calculation clearly identifies the massive

sulphide samples as having the most pentlandite, up to the upper bound of 0.3 vol. fraction, with correspondingly minimal silicate content, down to 0 vol. fraction. As the predicted sulphide content goes up, the predicted silicate content goes down.

There is significant variability in the heights of the bars in Figure 3, but there is much less variability in the position of the bottoms of the bars, or minimum abundances. These minimum abundances indicate what must be required to satisfy the imposed constraints, and can be used as an effective conservative estimate of mineral abundance. Our goal in this assessment is to correctly identify ore sulphide-bearing samples based on their physical properties. The samples most likely to contain pentlandite would be those where the minimum predicted abundance of pentlandite is > 0.001 volume fraction (the Δv threshold for significant figures defined above). Those most likely to contain ore sulphides (pyrrhotite + pentlandite) would have > 0.001 volume fraction pyrrhotite + pentlandite. These criteria are shown in Figure 4 where in each panel the samples have been sorted in order of increasing minimum ore sulphide content (top) or increasing minimum pentlandite content (bottom), with the 0.001 volume fraction cut-off identify by dashed line. The samples are coloured as in Figure 3, only their order has been changed. Immediately one can see that the barren and trace sulphides (blues) plot to the left, whereas the samples with higher actual sulphide contents plot to the right.

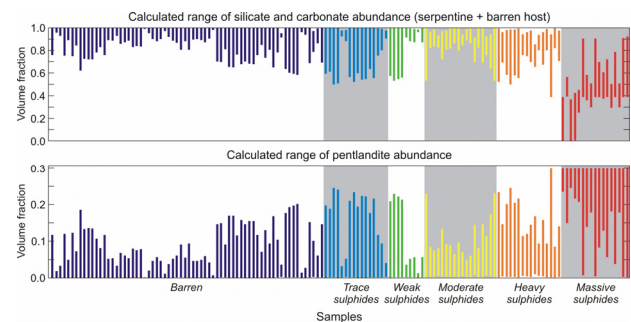


Figure 3: Results of the mineral estimate calculation on drill core samples from Leinster. Each vertical bar represents an individual sample and is coloured and grouped by its actual sulphide content. The tops and bottoms show the results obtained with each of the two objective functions thus defining the range of possibilities. As the actual sulphide content increases, the minimum abundance (bar bottoms) of pentlandite abundance tends to increase, and the maximum abundance (bar tops) of silicate and carbonate abundance tends to decrease.

Using these criteria we can test the accuracy of the mineral estimate prediction for barren and sulphide-bearing samples (Figure 5). A more conservative estimate would focus only on those samples that must contain pentlandite (Figure 4, bottom), however this will miss many of the pyrrhotite-rich samples that surround and are associated with ore. More than 85 % of barren samples are correctly predicted to be barren, and 81 % of sulphide-bearing samples are correctly predicted to contain sulphides. The success rate increases as the actual sulphide content increases. Using > 0.001 volume fraction pentlandite would reduce the number of false positives but increase the number of sulphide-bearing samples that are misidentified as barren.

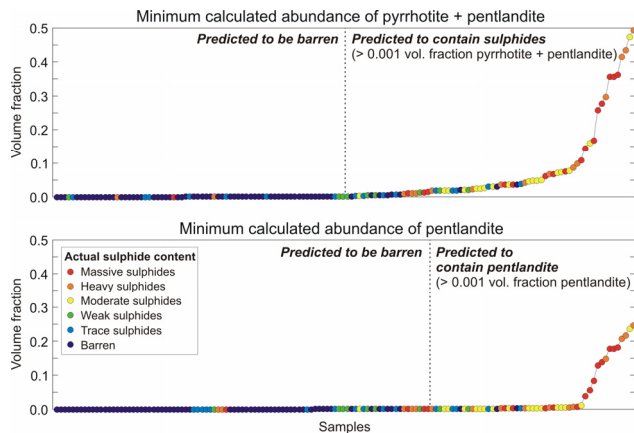


Figure 4: An alternate representation of the results from Figure 3. Here only the minimum abundances (bar bottoms) are shown (circles) coloured by actual sulphide content. The bars are sorted in order of increasing minimum predicted abundance of pyrrhotite and pentlandite (top) or pentlandite alone (bottom). Where the respective predicted abundances exceed 0.001 volume fraction (depicted by dashed lines), the samples can be flagged as anomalous and worthy of follow-up. Either criteria can be used; for Figure 5 we use the pyrrhotite + pentlandite criteria to identify sulphide-bearing samples.

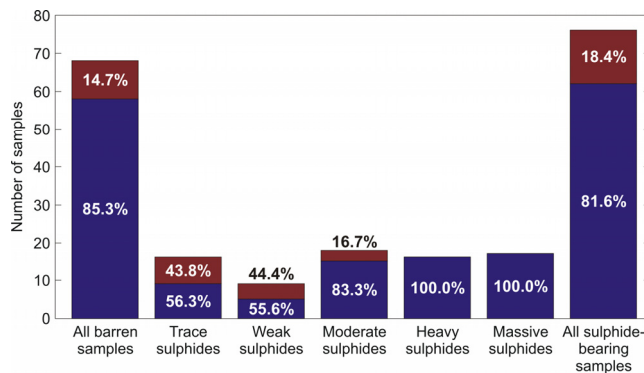


Figure 5: Graph showing the accuracy of the mineral predictions when using a cut-off of 0.001 volume fraction pyrrhotite and pentlandite (top of Figure 4). Each bar represents the listed group of samples based on visual estimates of sulphide content. Blue segments indicate the proportion of successful predictions for that group. Brown segments show where the predictions were incorrect, i.e., sulphide-bearing samples that were predicted to be barren (false negative) or barren samples predicted to contain sulphides (false positive).

Summary

The high success rate for identifying sulphide-bearing samples based only on knowledge of densities and susceptibilities is very encouraging. Using a cut-off criterion based on the minimum abundance of ore sulphides results in minimal false positives, where barren rocks are incorrectly identified as sulphide-bearing, yet has a high success rate at identifying actual sulphide-bearing rocks.

APPLICATION TO 3D INVERSION MODELS

In practice the mineral estimates are better suited to situations where visual inspection of the rocks is impossible. One such situation might be where wireline downhole logs of density (or gamma-gamma density) and susceptibility have been recorded but core has been lost, has deteriorated, or is inaccessible. A more general application of the mineral estimates applies to densities and susceptibilities derived for the subsurface using geophysical modelling and inversion techniques.

Gravity and magnetic inversions are becoming standard practice in many mineral exploration programs and are one of the few ways in which 3D information can be inferred from buried rocks. Interpreting the 3D density and magnetic susceptibility models derived using inversions is challenging due to the number of factors that can influence the physical properties of a particular rock or rock type. Measurements of physical properties on samples can supply some information on the physical properties expected for particular rocks and alteration or mineralisation styles. However, in ancient or complex hydrothermal and metamorphic terrains such measurements may not be representative of all possible geological processes in the region, and the rocks may be deeply buried preventing direct access and measurement anyway. In such scenarios, an estimate of mineralogy derived from inferred physical properties, a general understanding of the processes the rocks may have been exposed to, and knowledge of ore deposit models may provide a useful targeting tool for focusing future exploration efforts.

Olympic Dam

Here we present an example of how the mineral estimation can be applied to the results of regional-scale gravity and magnetic inversions over the Olympic Cu-Au province north of Adelaide along the eastern margin of the Gawler Craton in South Australia. Despite negligible Proterozoic outcrop, and thick Proterozoic to Cambrian basinal cover sequences, it is highly prospective for Proterozoic Cu-Au mineralisation. It hosts the giant Olympic Dam iron oxide Cu-Au-U-Ag-REE (IOCG) deposit which contains total resources of 4430 Mt at 1.1 % Cu, 0.4 kg/t U₃O₈, 0.5 g/t Au, and 2.2 g/t Ag (BHP Billiton Ltd., 2006), as well as two significant new IOCG discoveries in the last decade at Prominent Hill (Belperio and Freeman, 2004) and Carrapateena (Fairclough, 2005), northwest and south, respectively, of this study's area of interest. Olympic Dam consists of a large (> 3 km diameter) accumulation of hematite-chalcopyrite-bornite-magnetite mineralisation hosted by a 7 km × 5 km areal extent breccia complex within a granitic batholith, below a minimum of 260 m of younger transported cover rocks (Reeve et al., 1990; Skirrow et al., 2002). The batholith is one of several large Paleoproterozoic to Mesoproterozoic granitoid suites in the Olympic province, which also includes a core of Archean granulite facies rocks underlying various metamorphosed volcanic and sedimentary sequences intruded by or associated with the granitoid suites (Daly et al., 1998).

Gravity and magnetic inversions were prepared by Williams et al. (2004) using the UBC-GIF inversions software GRAV3D and MAG3D (Li and Oldenburg, 1996, 1998) and publicly available regional gravity and magnetic data (Geophysical

Archive Data Delivery System: <http://www.geoscience.gov.au/gadds/>). These inversions covered a region of 150 km × 150 km to a depth of 10 km centered on the Olympic Dam deposit, and used 1 km × 1 km and 0.5 km tall cells (0.5 km³) throughout. As described by Williams et al. (2004), a basic reference model of expected geology, based on the basement geology interpretation by Direen and Lyons (2002) was used to constrain the inversions and physical properties were defined for each of the 10 rock units in the model based on physical property measurements on drill core samples (N. Direen, unpub. data, 2002).

The goal of our present study is to assess whether mineralogical maps can be derived from density and magnetic susceptibility models recovered by the inversions and whether such maps might add value to the recovered inversion results. Our study was not seeking to identify candidate exploration targets and no ground validation of the results has been conducted except by correlation with the locations of known copper deposits and prospects. The work presented here should be considered a proof of concept rather than a formal exploration outcome for the Olympic Cu-Au province.

Estimating mineral abundances from inversion models

Component properties

Mineralogy estimates can be obtained from density and magnetic inversion models using a similar approach to that described above for drill core samples. For IOCG systems the dominant minerals controlling the physical properties of the rocks will be magnetite, hematite, chalcopyrite, pyrite, and the low density alteration phase sericite, plus the barren host rock component that contains all other silicate and carbonate minerals. The properties of these minerals are outlined in Table 3. Although generally a mixture of white micas with densities of 2.7-3.0 g/cm³ (Chesterman and Lowe, 1979), intensely sericitised rocks are likely to have lower densities due to increased porosity as a result of mass loss to the acidic fluids responsible for the sericitisation. Table 3 therefore shows our estimated properties for intensely sericitised rocks in this region.

For an unaltered or minimally altered rock the primary control on the rock's physical properties is its lithology. In a geologically-constrained potential field inversion the user will have supplied a 3D model of expected physical properties for each cell to guide the inversion towards a solution that is consistent with the geology. This 3D reference model will be based on any existing knowledge of the geology of the area, including mapping, drilling, structural interpretation and conceptual models. The inversion will recover a physical property model that is as close as possible to the reference model while still reproducing the observed geophysical data. Due to the size of the model, the size of the cells, and the lack of detailed knowledge of the true geology within the model, the reference model will only represent coarse-scale geological features, > 10-20 km across at the scale of this study, and is unlikely to represent more localised hydrothermal alteration and mineralisation. The densities defined in the reference model, $\bar{\rho}_{host}$, can therefore be used as an estimate of the barren host rock properties for each inversion cell. The range of

susceptibilities is defined by the range of susceptibilities expected for rocks containing only silicate and carbonate minerals.

Uncertainties

When applied to drill core samples (above), uncertainties associated with the physical properties of minerals, barren host rock component, or samples could readily be defined in terms of measurement ranges or standard deviations. The inversion cells are orders of magnitude larger than the individual core samples that actual property measurements were made on so it is necessary to adjust the uncertainties to allow for the volume scaling of variance. A geostatistical analysis of a large physical property database would provide an understanding of the magnitude of the reduction in variance for a particular suite of rocks, but such data is rarely available at the scale (up to 10s or 100s of kilometres) of inversion models.

The range of allowable host rock end-member densities, $\bar{\rho}_{host} \pm \Delta \rho_{host}$, will be reduced by bulk averaging of the rock and will converge towards the mean rock density, $\bar{\rho}_{host}$, with increasing cell volumes. The value of $\Delta \rho_{host}$ can therefore be reduced for large cell volumes.

The uncertainty in the accuracy of the physical properties recovered by the inversion is more problematic. The reduction in variance associated with increasing rock volumes would be partially compensated for by an increase in the uncertainty associated with the physical properties recovered by inversion compared to direct measurement.

Objective functions

Two objective functions are defined to extract a possible range of mineral abundances with one extreme represented by the maximum possible abundance of the copper ore chalcopyrite

$$F_1(\mathbf{x}) = \mathbf{c}^T \mathbf{x} = x_{mgt} + x_{hem} - x_{cpy} + x_{py} + x_{ser} + x_{host}, \quad (21)$$

and the other represented by the maximum abundance of the barren host rock component

$$F_2(\mathbf{x}) = \mathbf{c}^T \mathbf{x} = x_{mgt} + x_{hem} + x_{cpy} + x_{py} + x_{ser} - x_{host}. \quad (22)$$

Additional constraints

Since no information is available regarding the absolute maximum and minimum abundances of each of the six components within 0.5 km³ cells, default lower and upper bounds of 0 and 1, respectively, are used for each component. One additional constraint is included based on the premise that alteration is more common than mineralisation. In particular it is expected that the amount of chalcopyrite will always be less than the amount of hematite in any sample (Reeve et al., 1990), so we apply a constraint of the form

$$x_{cpy} \leq x_{hem}. \quad (23)$$

Table 3: Summary of the physical properties of common minerals associated with iron oxide copper gold (IOCG) deposits. Where conflicting ranges are reported in the literature, a representative range is used.

Mineral	Minimum density (g/cm ³)	Maximum density (g/cm ³)	Minimum susceptibility (SI)	Maximum susceptibility (SI)	References
Sericite	2.10	2.30	1×10^{-5}	1×10^{-3}	Estimated (see text below)
Pyrite	5.00	5.04	3.50×10^{-5}	5.27×10^{-4}	Carmichael (1982), Hunt et al. (1995)
Chalcopyrite	4.18	4.22	2.30×10^{-5}	4.02×10^{-4}	Hunt et al., (1995)
Hematite	5.24	5.30	1.00×10^{-4}	4.02×10^{-2}	Carmichael (1982), Hunt et al. (1995)
Magnetite	5.10	5.20	3	8	Telford et al. (1990), Clark (1997)

Results

In general the method is unable to clearly differentiate between chalcopyrite-, pyrite-, and hematite-bearing rocks at the scale of 0.5 km³ inversion model cells. This might be expected based on the IOCG ore deposit model and the constraint imposed by equation 23, but is also an artefact of the scale of observation and minimising the objective functions. The calculation is more likely to include hematite to explain a dense cell as the volume of the higher density hematite required to explain the high density cell is lower than the volume of the lower density chalcopyrite and pyrite required. Since IOCG ore bodies commonly contain all three minerals we usually display images of hematite + sulphide abundance which will effectively identify the more volumetrically extensive hematite alteration zones that might contain and enclose IOCG mineralisation. Despite the lack of resolution of the individual minerals in this example, the result is more accurate than including a combined hematite-pyrite-chalcopyrite end-member that would have extremely broad uncertainty in its expected physical properties of 4.18-5.3 g/cm³ and 2.30×10^{-5} to 4.02×10^{-2} SI (from Table 3).

The maps in **Figure 6** show calculated abundances of magnetite, sericite, and hematite + sulphide at the inferred basement surface derived from drill hole intersections. Following the method used for drill core samples above where the minimum calculated abundances were used to provide an effective conservative estimate of sulphide content, we will focus on the minimum calculated hematite + sulphide abundances for the Olympic province inversions obtained when the abundance of barren host rock is maximised. This identifies areas where the supplied reference model of properties and therefore the available geological understanding, and the supplied constraints are insufficient to explain the gravity and magnetic anomalies, and so some hematite and sulphides are required.

In **Figure 6**, the largest and richest hematite and sulphide calculated anomaly exactly coincides with the Olympic Dam deposit, but the calculation also identified potential hematite and sulphide accumulations near several other copper prospects. Some prospects do not show evidence of hematite and sulphide accumulations in this calculation, but are associated with anomalous magnetite accumulations; these may represent low-grade copper targets, or prospects where copper zones lie below the inferred basement surface. There are also

some areas that show potential for hematite and sulphides where no known copper has been identified during previous exploration; these may represent hematite-rich rocks with no copper sulphides, areas where the geological understanding is incorrect, or genuine prospective targets.

By converting the physical properties recovered by the inversion into a mineralogical model the results can be interpreted and prospective areas ranked with respect to the IOCG mineral system model. High quality targets will have larger, richer predicted accumulations of hematite and sulphides within or adjacent to magnetite accumulations (Bastrakov et al., 2002), possibly with local sericite alteration. Lower quality targets might have small or less abundant hematite and sulphide zones or greater separation from adjacent magnetite accumulations.

CONCLUSIONS

Reliable estimates of mineral abundances can be extracted from physical property measurements by including an understanding of the minerals most likely to control the physical properties of the rocks, a small number of geological constraints, and allowing for measurement uncertainty. Maps of the extracted minimum abundances provide realistic first-pass estimates of the distribution of minerals at depth and under cover when applied to geologically-constrained gravity and magnetic inversion results. These results can help identify target areas for further data acquisition or sampling when interpreted with an understanding of likely ore deposit models. The accuracy of the maps depends on

- the quality and resolution of the gravity and magnetic data,
- the accuracy of the geologic reference model used to constrain the inversions,
- the resolution of the inversions,
- how representative the selected suite of minerals or components is,
- the accuracy of lower and upper bounds on mineral abundances,
- the accuracy of the mineralogical constraints used, and
- the level of uncertainty allowed in the calculation.

If improvements can be made at any of these stages, such as developing an improved geological understanding after drilling a hole, then those improvements should be included in an updated iteration of the mineral estimation process.

As these estimates are based on only two data they are underdetermined, and the extracted range of possible mineral

abundances may be large. The best solution to this problem is to include additional data. An unlimited number of geophysical or geological datasets can be included in the calculation by adding equations similar to equations 9 and 10. These will make the calculation less underdetermined and enhance the resolution of each end-member component. Obvious candidate datasets include resistivity or conductivity, chargeability, and

seismic velocities. Unfortunately many of these datasets may have nonlinear relationships to mineral abundances, and depend on characteristics other than mineral abundances, such as the connectivity of conductive minerals. Such complexities may require the use of nonlinear, or quadratic, programming techniques.

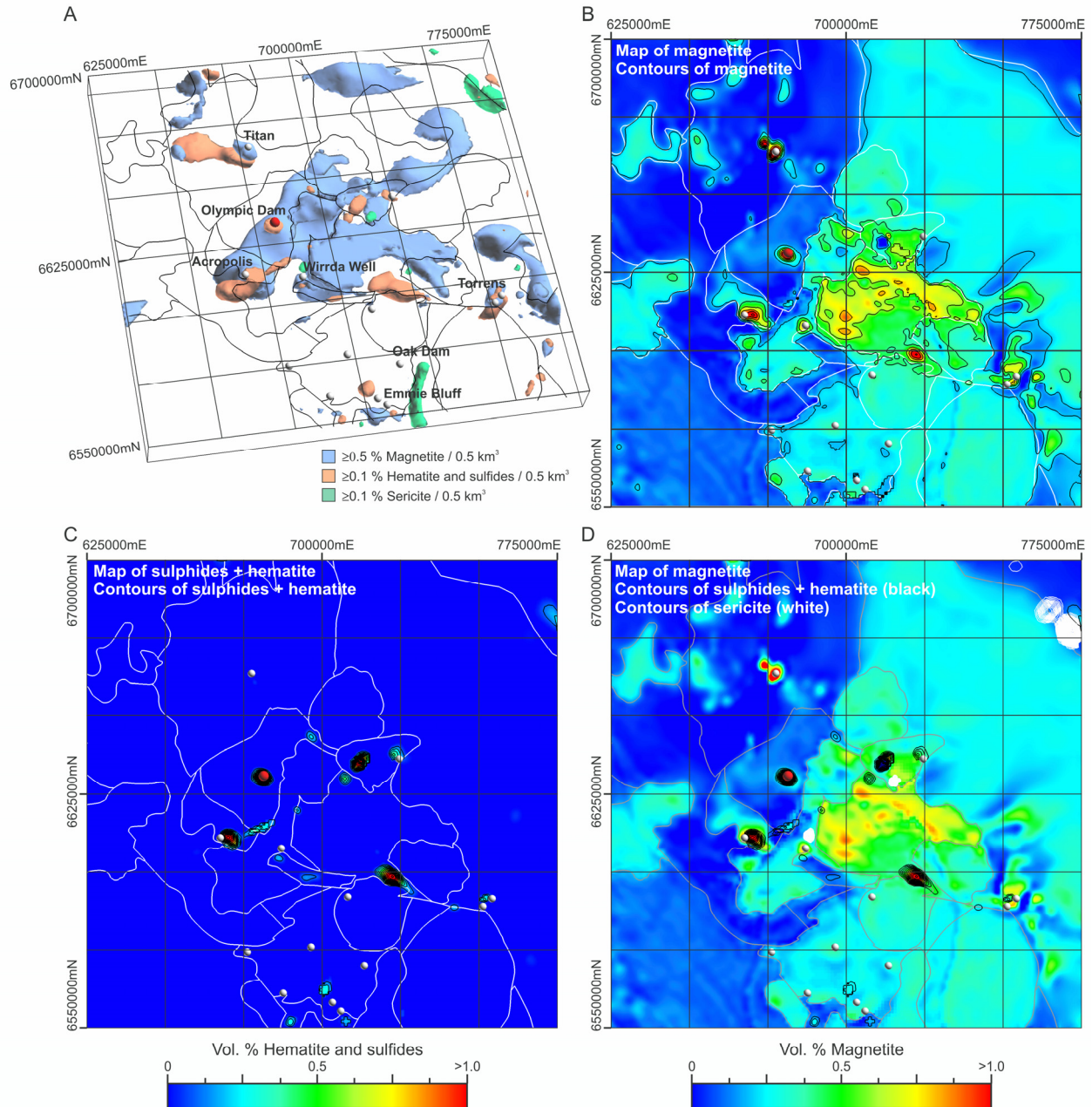


Figure 6: A. Perspective view of a 3D alteration map of the inversion volume. Brown surfaces enclose all cells with > 0.1 vol. % hematite or sulphides; green surfaces enclose cells with > 0.1 vol. % sericite; blue surfaces enclose cells with > 0.5 vol. % magnetite. Black lines indicate unit boundaries used in reference model; red spheres indicate mines/deposits, small spheres indicate prospects/occurrences, with the main occurrences labelled. B. Calculated magnetite abundance on the basement surface with 0.2% contours of magnetite shown in black, and unit boundaries shown in white. C. Calculated hematite + sulphide abundance on the basement surface with 0.1% contours of hematite + sulphides shown in black and unit boundaries shown in white. D. Calculated magnetite abundance on the basement surface with 0.1% contours of hematite + sulphides shown in black, 0.1% contours of hematite + sulphides shown in white, and unit boundaries shown in grey.

ACKNOWLEDGEMENTS

This work is part of a collaborative research project between the Mineral Deposit Research Unit and the Geophysical Inversion Facility at The University of British Columbia. The project was funded by Anglo American, Anglo Gold Ashanti, Barrick Gold Corp., BHP Billiton, CVRD Inco, Geoinformatics Exploration, Kennecott Exploration, Teck Cominco, Xstrata, and the NSERC CRD and Discovery Grants programs. BHP Billiton is thanked for access and support for the Leinster work. The Leinster physical property analyses were funded by a grant from the Society of Economic Geologists; Mike Smith at Geoscience Australia is thanked for performing the density analyses, and Chris Klootwijk and Brad Pillans at the Australian National University Palaeomagnetic Laboratory are thanked for training and assistance in measuring the susceptibilities. We thank William Morris for his review of the manuscript. Geoscience Australia and the Predictive Mineral Discovery Cooperative Research Center are thanked for their support of NW. NW publishes with the permission of the CEO of Geoscience Australia

REFERENCES

- Barnes, S. J., R. E. T. Hill, and M. J. Gole, 1988, The Perseverance ultramafic complex, Western Australia; the product of a komatiite lava river: *Journal of Petrology*, 29, 305-331.
- Bastrakov, E. N., R. G. Skirrow, and K. M. Barovich. 2002. Towards discriminating Cu-Au mineralised from barren hydrothermal systems using fluid chemistry: Gawler Craton 2002 - State of Play, 5-6 December, Adelaide.
- Belperio, A., and H. Freeman, 2004, Common geological characteristics of Prominent Hill and Olympic Dam; implications for iron oxide copper-gold exploration models: *AusIMM Bulletin*, 6, 67-75.
- BHP Billiton Ltd., 2006, 2006 BHP Billiton Annual Report: BHP Billiton Ltd.
- Bleil, U., and N. Petersen, 1982, Magnetic properties of natural minerals, in Angenheister, G., ed., *Physical properties of rocks*, Vol. 1b: Springer-Verlag, 308-365.
- Boardman, J. W., F. A. Kruse, and R. O. Green, 1995, Mapping target signatures via partial unmixing of AVIRIS data: *Proceedings of the Fifth JPL Airborne Earth Science Workshop*, JPL Publication 95-1, 1, 23-26.
- Carmichael, R. S., 1982, *Magnetic properties of minerals and rocks*: CRC Press.
- Chesterman, C. W., and K. E. Lowe, 1979, *The Audubon Society field guide to North American rocks and minerals*: Alfred A. Knopf.
- Clark, D. A., 1997, Magnetic petrophysics and magnetic petrology: aids to geological interpretation of magnetic surveys: *AGSO Journal of Australian Geology and Geophysics*, 17, 83-103.
- Daly, S. J., C. M. Fanning, and M. C. Fairclough, 1998, Tectonic evolution and exploration potential of the Gawler Craton, South Australia: *AGSO Journal of Australian Geology and Geophysics*, 17, 145-168.
- Direen, N., and P. Lyons, 2002, Geophysical interpretation of the Central Olympic Cu-Au province, 1:500,000 scale map sheet: Geoscience Australia.
- Duuring, P., W. Bleeker, and S. W. Beresford, 2007, Structural modification of the komatiite-associated Harmony nickel sulphide deposit, Leinster, Western Australia: *Economic Geology*, 102, 277-297.
- Emerson, D. W., K. Martin, and P. K. Williams, 1999, Electrical, magnetic and mass properties of the nickeliferous komatiite sequence near Leinster, Western Australia: *Preview*, 81, 13-22.
- Fairclough, M., 2005, Geological and metallogenic setting of the Carrapateena FeO-Cu-Au prospect; a PACE success story: *MESA Journal*, 38, 4-7.
- Fukuda, K., and A. Prodon, 1996, Double description method revisited, in Deza, M., R. Euler, and I. Manoussakis, eds., *Combinatorics and computer science*: Springer, 91-111.
- Gole, M. J., S. J. Barnes, and R. E. T. Hill, 1989, The geology of the Agnew nickel deposit, Western Australia: *CIM Bulletin*, 82, 46-56.
- Gordon, T. M., and G. M. Dipple, 1999, Measuring mineral abundance in skarn; II, A new linear programming formulation and comparison with projection and Rietveld methods: *The Canadian Mineralogist*, 37, 17-26.
- Hanneson, J. E., 2003, On the use of magnetics and gravity to discriminate between gabbro and iron-rich ore-forming systems: *Exploration Geophysics*, 34, 110-113.
- Henkel, H., 1976, Studies of density and magnetic properties of rocks from northern Sweden: *Pure and Applied Geophysics*, 114, 235-249.
- Henkel, H., 1994, Standard diagrams of magnetic properties and density; a tool for understanding magnetic petrology: *Journal of Applied Geophysics*, 32, 43-53.
- Hunt, C. P., B. M. Moskowitz, and S. K. Banerjee, 1995, Magnetic properties of rocks and minerals: *AGU Reference Shelf*, 3, 189-204.
- Li, Y., and D. W. Oldenburg, 1996, 3-D inversion of magnetic data: *Geophysics*, 61, 394-408.
- Li, Y., and D. W. Oldenburg, 1998, 3-D inversion of gravity data: *Geophysics*, 63, 109-119.
- Libby, J. W., P. R. Stockman, K. M. Cervo, M. R. K. Muir, M. Whittle, and P. J. Langworthy, 1998, Perseverance nickel deposit, in Berkman, D. A., and D. H. Mackenzie, eds., *Geology of Australian and Papua New Guinean mineral deposits*: Australasian Institute of Mining and Metallurgy, 321-328.
- Martin, J. E., and P. D. Allchurch, 1975, Perseverance nickel deposit, Agnew, in Knight, C. L., ed., *Economic geology of Australia and Papua New Guinea, 1. Metals*: Australasian Institute of Mining and Metallurgy, 149-155.
- Motzkin, T. S., H. Raiffa, G. L. Thompson, and R. M. Thrall, 1953, The double description method, in Kuhn, H. W., and A. W. Tucker, eds., *Contributions to theory of games*, Vol. 2: Princeton University Press, 51-73.
- Puranen, R., 1989, Susceptibilities, iron and magnetite content of Precambrian rocks in Finland: Tutkimusraportti - Geologian Tutkimuskeskus = Report of Investigation - Geological Survey of Finland.

- Reeve, J. S., K. C. Cross, R. N. Smith, and N. Oreskes, 1990, Olympic Dam copper-uranium-gold-silver deposit, in Hughes, F. E., ed., *Geology of the mineral deposits of Australia and Papua New Guinea*, v. 2: The Australian Institute of Mining and Metallurgy, 1009-1035.
- Schön, J. H., 2004, *Physical properties of rocks: Fundamentals and principles of petrophysics*: Elsevier.
- Skirrow, R. G., E. Bastrakov, G. J. Davidson, O. L. Raymond, and P. Heathersay, 2002, The geological framework, distribution and controls of Fe-oxide Cu-Au mineralisation in the Gawler Craton, South Australia: Part II - Alteration and mineralisation, in Porter, T. M., ed., *Hydrothermal iron oxide copper-gold & related deposits: A global perspective*, volume 2: PGC Publishing, 33-47.
- Smith, M. O., P. E. Johnson, and J. B. Adams, 1985, Quantitative determination of mineral types and abundances from reflectance spectra using principal components analysis: Proceedings of the Fifteenth Lunar and Planetary Science Conference, Part 2, *Journal of Geophysical Research*, 90 (Supplement), C797-C804.
- Telford, W. M., L. P. Geldart, and R. E. Sheriff, 1990, *Applied Geophysics*, 2nd ed: Cambridge University Press.
- Theseira, M. A., G. Thomas, J. C. Taylor, F. Gemell, and J. Varjo, 2003, Sensitivity of mixture modelling to end-member selection: *International Journal of Remote Sensing*, 24, 1559-1575.
- Torrisi, F., and M. Baotic, 2005, CDDMEX - Matlab interface for the CDD solver: <http://control.ee.ethz.ch/~hybrid/cdd.php>.
- Van der Meer, F., and S. M. De Jong, 2000, Improving the results of spectral unmixing of Landsat Thematic Mapper imagery by enhancing the orthogonality of end-members: *International Journal of Remote Sensing*, 21, 2781-2797.
- Williams, N. C., R. Lane, and P. Lyons, 2004, Towards 3D maps of alteration under cover: Regional constrained 3D inversion of potential field data from the Olympic Cu-Au province, South Australia: *Preview*, 30-33.
- Wohlenberg, J., 1982, Density of minerals, in Angenheister, G., ed., *Physical properties of rocks*, Vol. 1b: Springer-Verlag, 66-113.